Inactivating ion channels augment robustness of subthreshold intrinsic response dynamics to parametric variability in hippocampal model neurons

Rahul Kumar Rathour and Rishikesh Narayanan

Cellular Neurophysiology Laboratory, Molecular Biophysics Unit, Indian Institute of Science, Bangalore, India.

SUPPLEMENTAL DATA

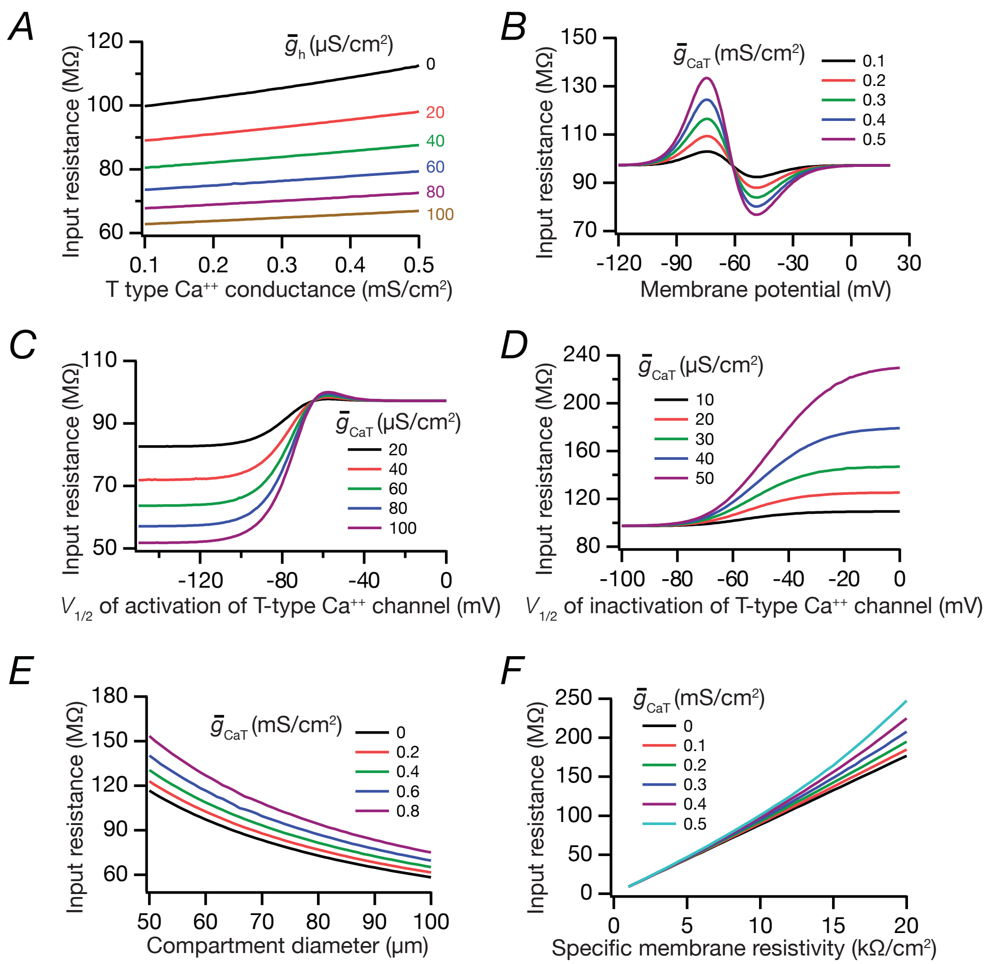

Supplementary Figure S1. Sensitivity analysis for parameters associated with a *T*-type Ca^{2+} conductance on input resistance. *A,* Increase in *T*-type Ca^{2+} conductance increased input resistance. *B,* Measuring input resistance at various membrane potentials in presence of I_{CaT} yielded a biphasic response. *C,* Depolarized shift in $V_{1/2}$ of activation of I_{CaT} increased input resistance. *D,* Depolarized shift in $V_{1/2}$ of inactivation of I_{CaT} increased input resistance. *E,* Increasing the compartment diameter decreased input resistance. *F,* Increasing the membrane resistivity increased input resistance.

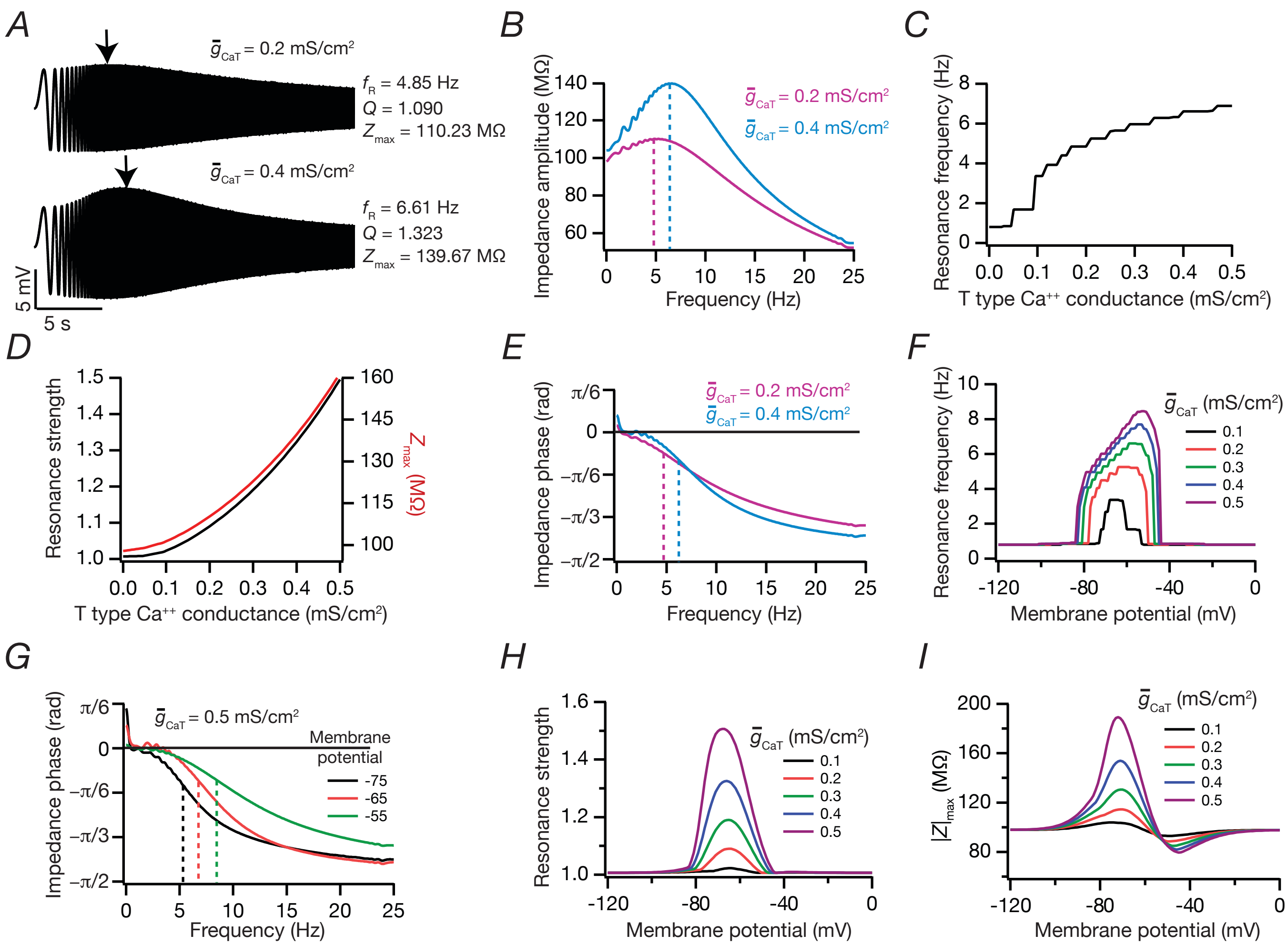

Supplementary Figure S2. Sensitivity analyses for parameters associated with *T*-type Ca^{2+} conductance on measurements related to intrinsic response dynamics. *A,* Voltage traces in response to chirp stimulus in presence of lower (top) and higher (bottom) magnitude of *T*-type Ca^{2+} conductances. *B,* Impedance amplitude plot derived from voltage traces shown in *A*. *C,* Increase in the magnitude of *T*-type Ca^{2+} conductance increased resonance frequency. *D,* Increase in the magnitude of *T*-type Ca^{2+} conductance increased resonance strength (black) and maximum impedance amplitude (red). *E,* Impedance phase plot derived from voltage traces shown in *A*. *F,* Plotting resonance frequency as a function of membrane potential, in presence of I_{CaT}, revealed a bell shaped dependence. *G,* Impedance phase plot at various membrane potentials showed no inductive lead. *H,* Measuring resonance strength at various membrane potentials in presence of I_{CaT} revealed a bell-shaped curve. *I,* Measuring maximum impedance amplitude at various membrane potentials in presence of I_{CaT} yielded an asymmetric biphasic curve.

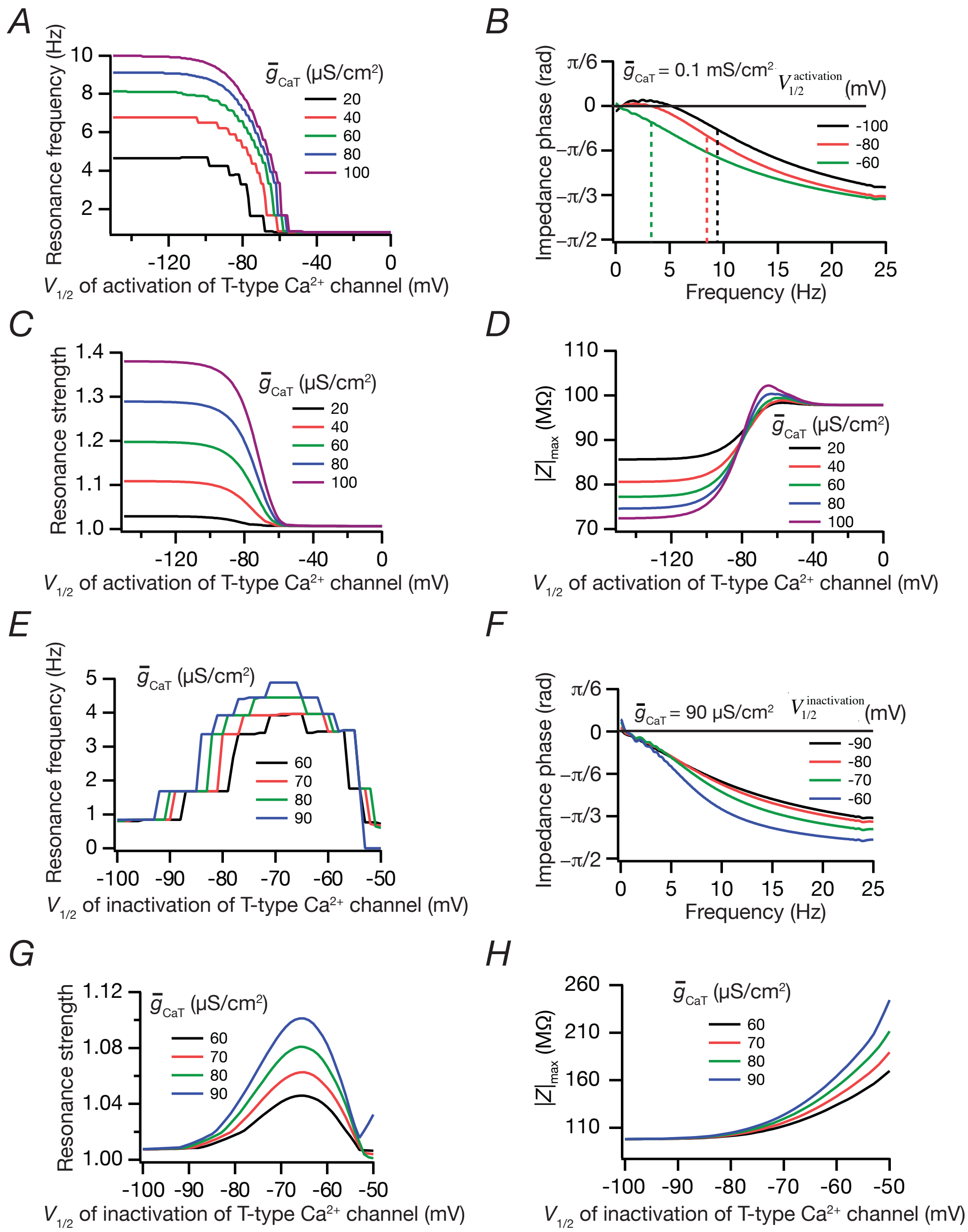

Supplementary Figure S3. Sensitivity analyses for $V_{1/2}$ of activation and inactivation of *T*-type Ca^{2+} conductance in determining measurements associated with intrinsic response dynamics. *A,* Hyperpolarized shift in $V_{1/2}$ of activation of I_{CaT} increased f_R. *B,* Impedance phase plot at various $V_{1/2}$ of activation potentials showed a very small lead component at hyperpolarized values of $V_{1/2}$ of activation. *C,* Hyperpolarized shift in $V_{1/2}$ of activation of I_{CaT} increased resonance strength. *D,* Hyperpolarized shift in $V_{1/2}$ of activation of I_{CaT} decreased maximum impedance amplitude. *E,* Measuring resonance frequency at various $V_{1/2}$ of inactivation potentials of I_{CaT} yielded a bell shaped curve. *F,* Impedance phase plot at various $V_{1/2}$ of inactivation potentials showed no lead. *G,* Measuring resonance strength at various $V_{1/2}$ of inactivation potentials of I_{CaT} yielded a bell shaped curve. *H,* Depolarized shift in $V_{1/2}$ of inactivation of I_{CaT} increased maximum impedance amplitude.

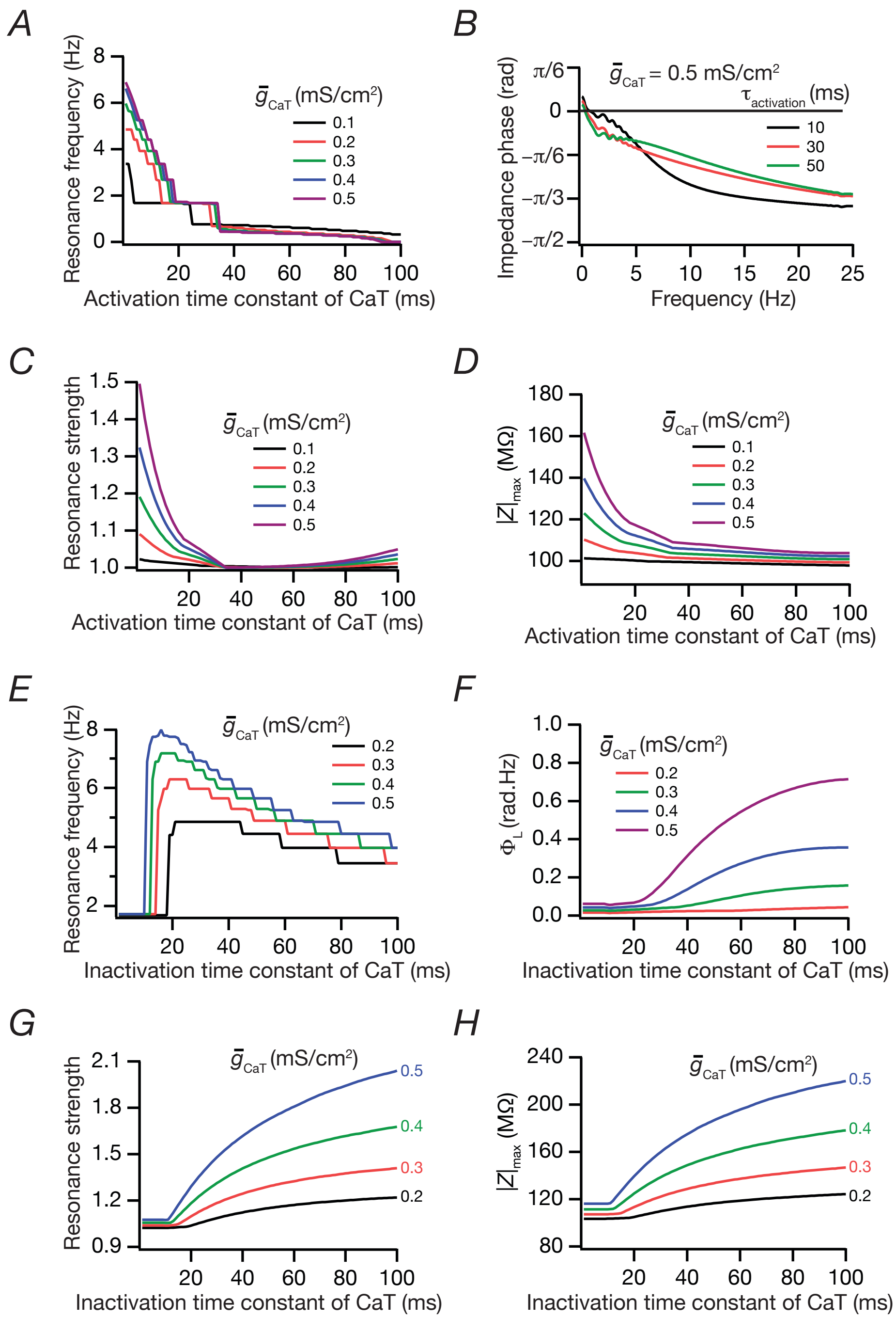

Supplementary Figure S4. Sensitivity analyses for activation and inactivation time constants of *T*-type Ca^{2+} conductance in regulating measurements related to intrinsic response dynamics. *A,* An increase in activation time constant of I_{CaT} led to a decrease in resonance frequency. *B,* Impedance phase plot at various activation time constant of I_{CaT} showed no inductive lead. *C,* An increase in activation time constant of I_{CaT} led to a decrease in resonance strength. *D,* An increase in activation time constant of I_{CaT} led to a decrease in maximum impedance amplitude. *E,* An increase in inactivation time constant (after crossing a certain threshold for resonance to occur) of I_{CaT} resulted in a decrease in resonance frequency. *F,* An increase in inactivation time constant (after crossing a certain threshold for resonance to occur) of I_{CaT} resulted in an increase in total inductive phase. *G,* An increase in inactivation time constant (after crossing a certain threshold for resonance to occur) of I_{CaT} led to an increase in resonance strength. *H,* An increase in inactivation time constant (after crossing a certain threshold for resonance to occur) of I_{CaT} led to an increase in maximum impedance amplitude.

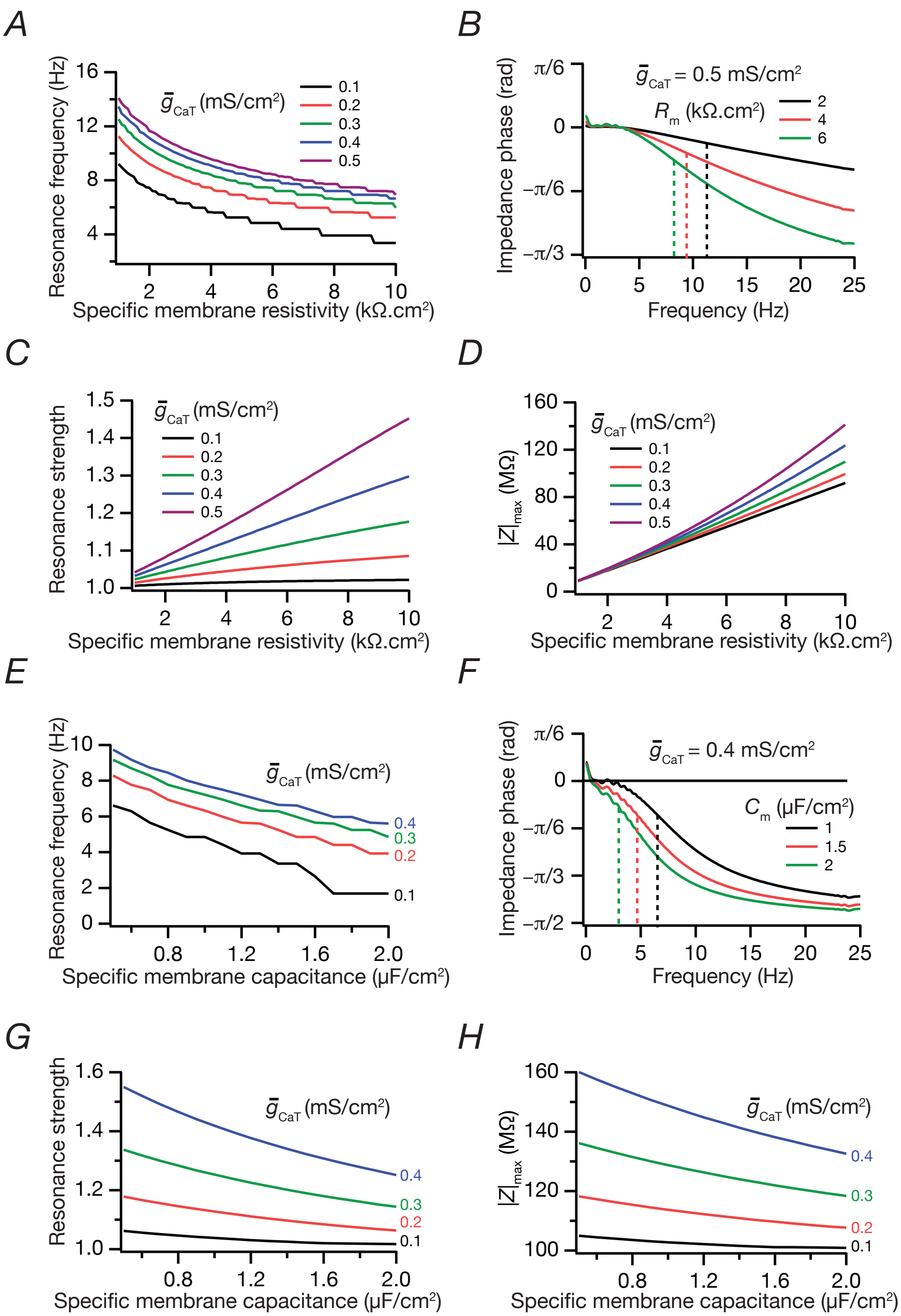

Supplementary Figure S5. Sensitivity analysis for passive properties in regulating measurements of intrinsic response dynamics that are mediated by *T*-type Ca^{2+} conductance. *A,* An increase in membrane resistivity led to a reduction in resonance frequency. *B,* Impedance phase plot at various values of membrane resistivity showed no inductive lead. *C,* An increase in membrane resistivity led to an increase in resonance strength. *D,* An increase in membrane resistivity led to an increase in maximum impedance amplitude. *E,* An increase in membrane capacitance led to a reduction in resonance frequency. *F,* Impedance phase plot at various values of membrane capacitance showed no inductive phase lead. *G,* An increase in membrane capacitance led to a reduction in resonance strength. *H,* An increase in membrane capacitance led to a reduction in maximum impedance amplitude.

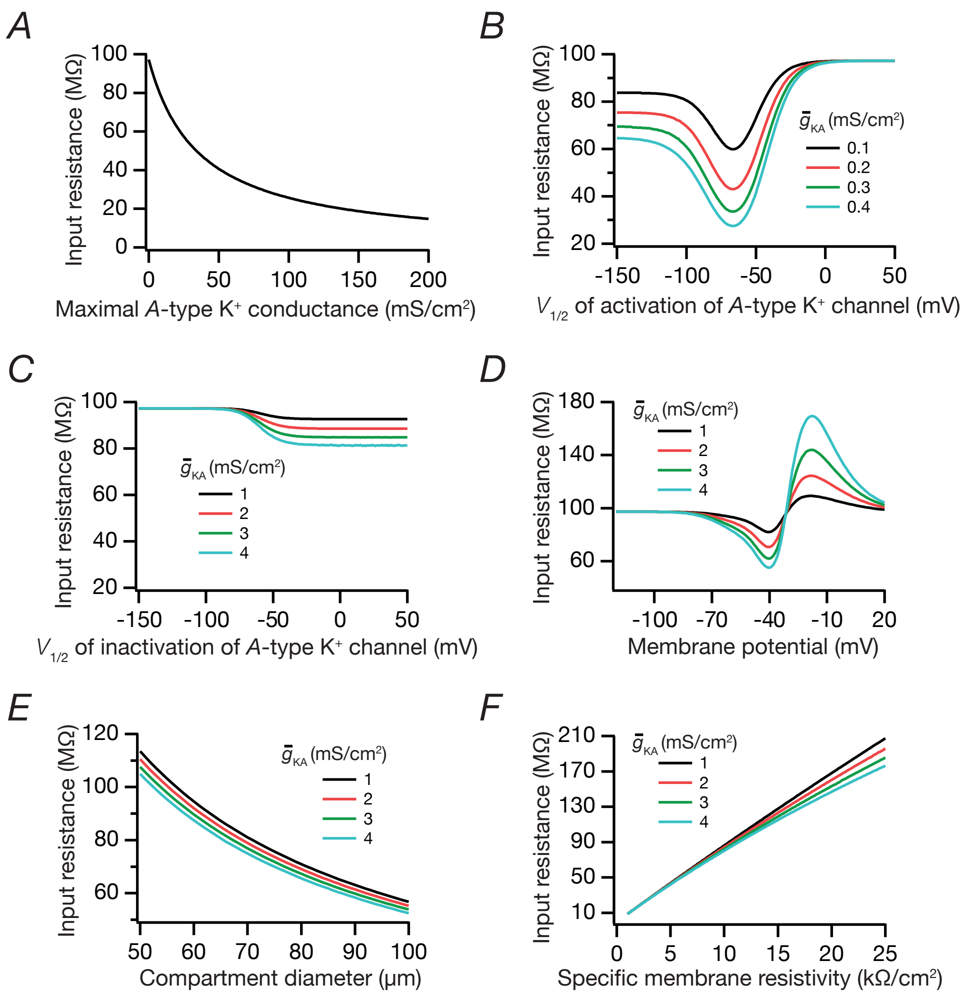

Supplementary Figure S6. Sensitivity analyses for parameters associated with an *A*-type K$^+$ conductance on input resistance. *A,* Increase in *A*-type K$^+$ conductance decreased input resistance. *B,* Depolarized shift in $V_{1/2}$ of activation of I_{KA} yielded an asymmetric U-shaped curve for input resistance. *C,* Depolarized shift in $V_{1/2}$ of inactivation of I_{KA} decreased input resistance. *D,* Measuring input resistance at various membrane potentials in presence of I_{KA} revealted a biphasic dependence. *E,* Increasing the compartment diameter decreased input resistance. *F,* Increasing the membrane resistivity increased input resistance.

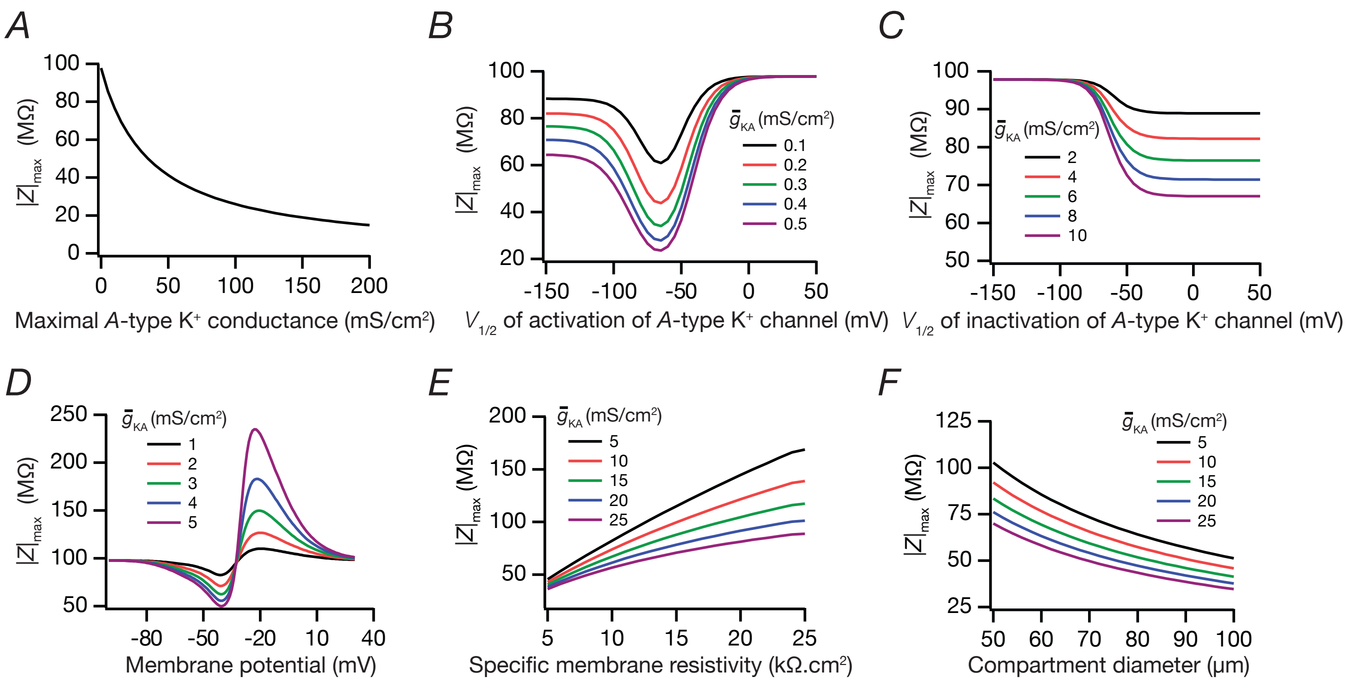

Supplementary Figure S7. Sensitivity analyses for parameters associated with an *A*-type K⁺ conductance on maximal impedence amplitude. *A,* Increase in *A*-type K⁺ conductances decreased maximal impedence amplitude. *B,* Depolarized shift in $V_{1/2}$ of activation of I_{KA} yielded an asymmetric U-shaped dependence for maximal impedence amplitude. *C,* Depolarized shift in $V_{1/2}$ of inactivation of I_{KA} decreased maximal impedence amplitude. *D,* Measuring maximal impedence amplitude at various membrane potentials in presence of I_{KA} yielded a biphasic response. *E,* Increasing the membrane resistivity increased maximal impedence amplitude. *F,* Increasing the compartment diameter decreased maximal impedence amplitude.

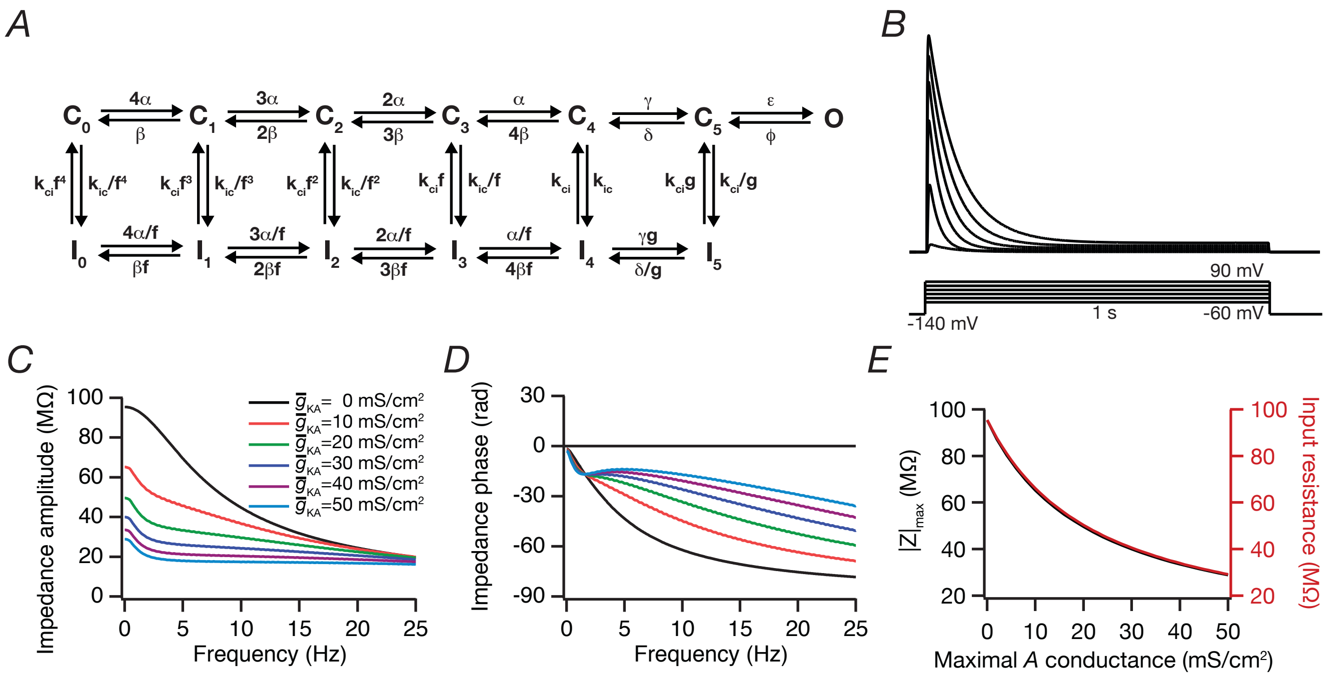

Supplementary Figure S8. Insertion of an *A*-type K$^+$ channel decreased $|Z|_{max}$ and R_{in}, apart from modulating the impedance phase profile. *A,* Multistate Markovian kinetic scheme used for modeling an *A*-type potassium channel, adopted from (Amarillo et al., 2008). *B,* Normalized current traces obtained for voltage-pulse protocols derived from the model shown in *A*. *C–D*, Impedance amplitude (*C*) and phase (*D*) profiles obtained when the *A*-type potassium channel, model shown in *A*, was inserted into a model neuron. The profiles are shown for various values of the maximal *A*-type potassium channel conductance. *E,* Plots depicting the relationships between maximal impedance amplitude and input resistance as functions of maximal *A* conductance. These were obtained from *C*.

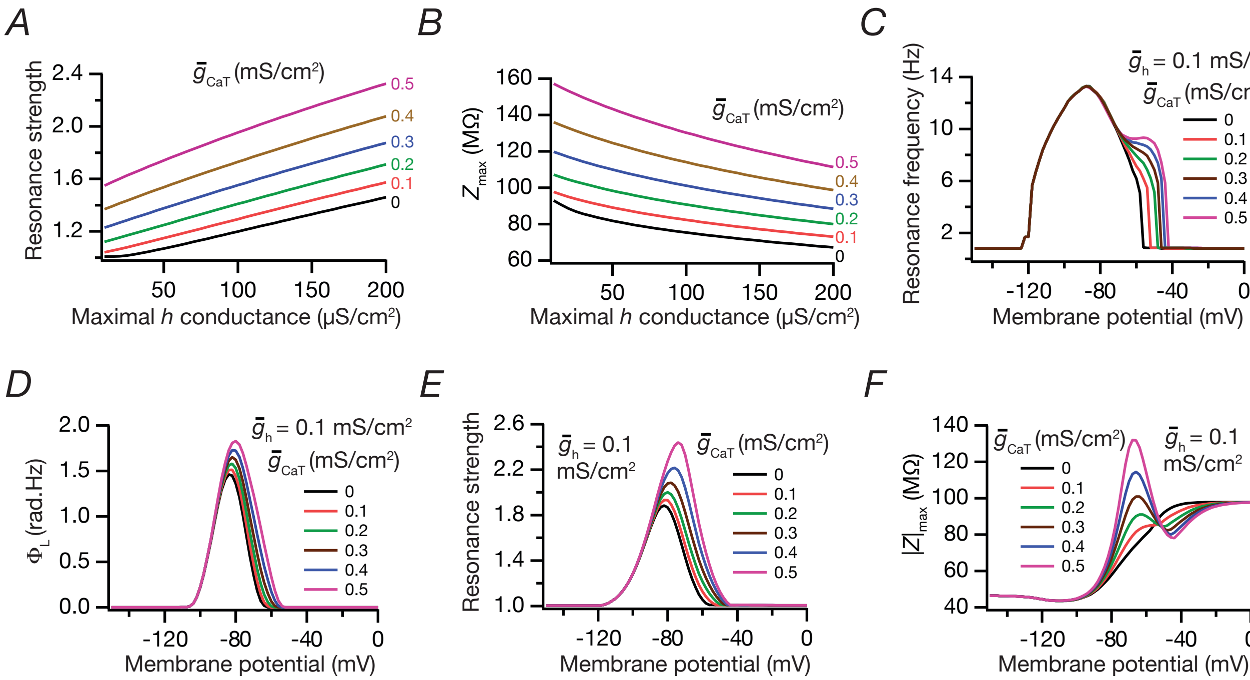

Supplementary Figure S9. Sensitivitiy analysis for the interaction between *h* conductance and *T*-type Ca^{2+} conductance in determining measurements related to intrinsic response dynamics. *A,* In the presence of an *h* conductance, increasing the magnitude of *T*-type Ca^{2+} conductance led to an increase in resonance strength. *B,* In the presence of an *h* conductance, increasing the magnitude of *T*-type Ca^{2+} conductance led to an increase in maximum impedance amplitude. *C,* Copresence of an *h* conductance with a *T*-type Ca^{2+} conductance enabled the system to sustain resonance at more depolarized potentials, where *h* conductance alone cannot sustain resonance. *D,* In the presence of *h* conductance, increasing the magnitude *T*-type Ca^{2+} conductance led to an increase in the total inductive phase at more depolarized potentials. *E,* In the presence of an *h* conductance, increasing the magnitude of *T*-type Ca^{2+} conductance led to an increase in resonance strength at more depolarized potentials. *F,* In the presence of an *h* conductance, increasing the magnitude *T*-type Ca^{2+} conductance led to an asymmetric biphasic curve for the maximum impedance amplitude.

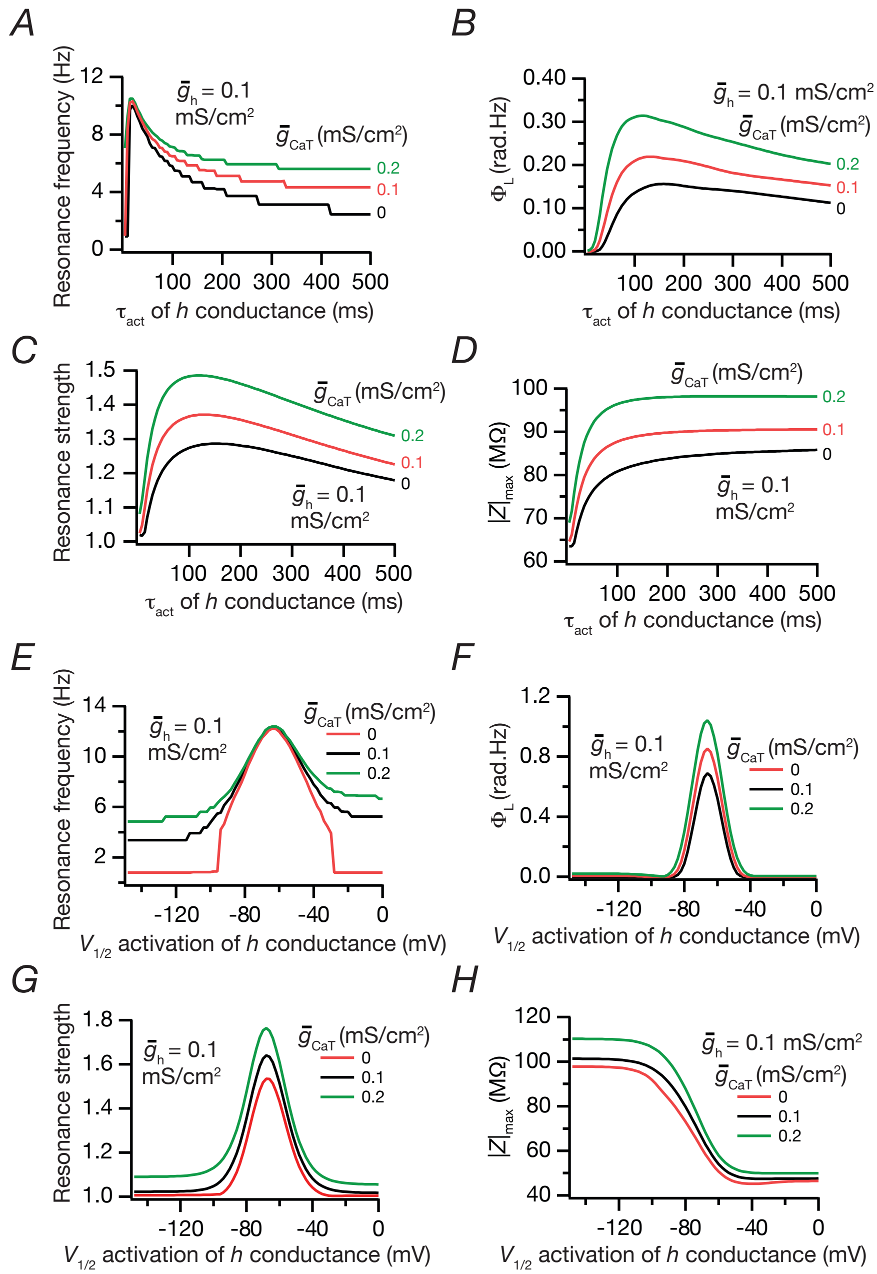

Supplementary Figure S10. Sensitivity analyses for active parameters associated with an *h* conductance on intrinsic response dynamics in the co-presence of a *T*-type Ca²⁺ conductance. *A,* An increase in activation time constant (after crossing a certain threshold for resonance to occur) of the *h* conductance led to a decrease in resonance frequency, irrespective of the presence of I_{CaT}. *B,* An increase in activation time constant (after crossing a certain threshold for resonance to occur) of the *h* conductance led to a small decrease in total inductive phase, irrespective of presence of I_{CaT}. *C,* An increase in activation time constant (after crossing a certain threshold for resonance to occur) of the *h* conductance led to a decrease in resonance strength, irrespective of presence of I_{CaT}. *D,* An increase in activation time constant (after crossing a certain threshold for resonance to occur) of the *h* conductance led to a small increase in maximum impedance amplitude, irrespective of presence of I_{CaT}. *E,* Resonance frequency at various $V_{1/2}$ activation potentials of the *h* conductance yielded bell-shaped dependencies. *F,* Total inductive phase at various $V_{1/2}$ activation potentials of the *h* conductance yided bell-shaped dependencies. *G,* Resonance strength at various $V_{1/2}$ activation potentials of the *h* conductance yielded bell-shaped dependencies. *H,* Maximum impedance amplitude at various $V_{1/2}$ activation potentials of the *h* conductance yielded a sigmoidal dependecies.

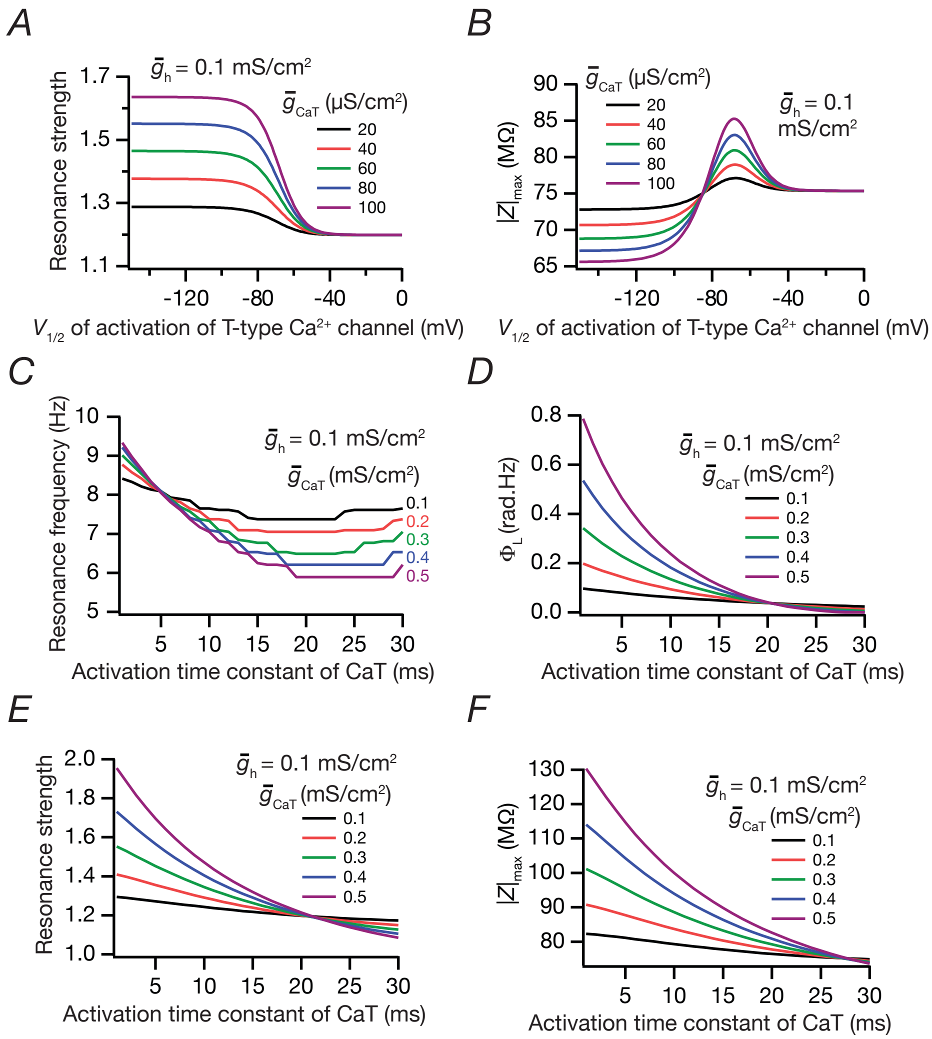

Supplementary Figure S11. Sensitivity analyses for the interactions between *h* conductance and active parameters of *T*-type Ca^{2+} conductance in determining resonance strength and maximum impedance amplitude. *A,* Hyperpolarized shift in $V_{1/2}$ of activation of I_{CaT} increased resonance strength. *B,* Hyperpolarized shift in $V_{1/2}$ of activation of I_{CaT} decreased maximum impedance amplitude. *C,* Increasing activation time constant of I_{CaT} decreased resonance frequency. *D,* Increasing activation time constant of I_{CaT} decreased total inductive phase. *E,* Increasing activation time constant of I_{CaT} decreased resonance strength. *F,* Increasing activation time constant of I_{CaT} decreased maximum impedance amplitude. All simulations were performed in the presence of a fixed magnitude of the *h* conductance.

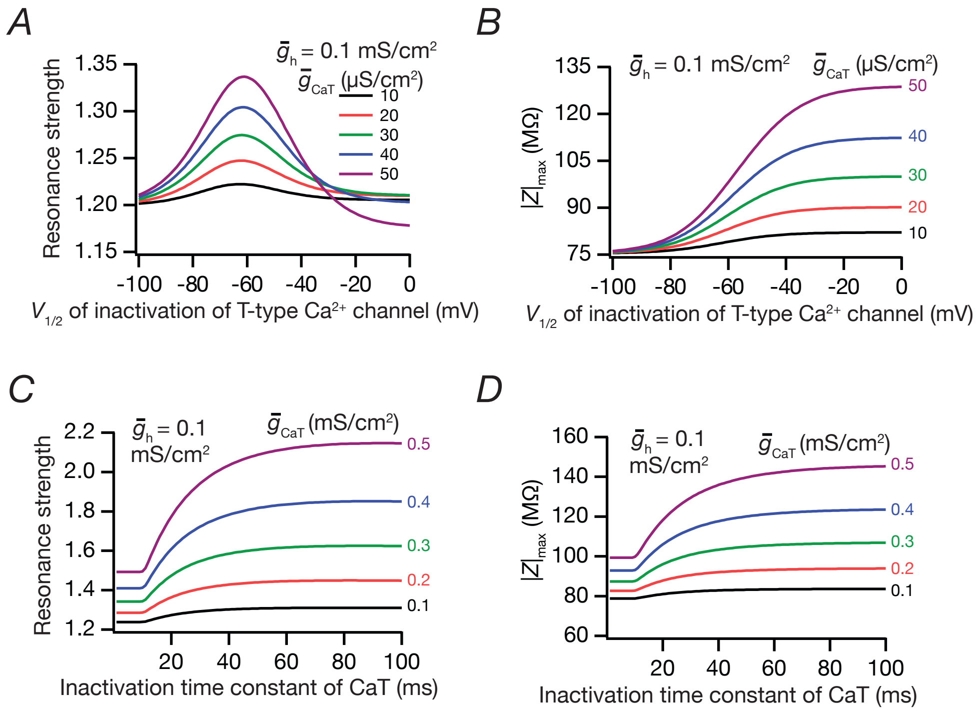

Supplementary Figure S12. Sensitivity analyses for half-maximal inactivation and inactivation time constants of *T*-type Ca^{2+} conductance on resonance strength and maximum impedance amplitude, in the presence of a *h* conductance. *A,* Depolarized shift in $V_{1/2}$ of inactivation of I_{CaT} yielded bell-shaped dependencices for resonance strength. *B,* Depolarized shift in $V_{1/2}$ of inactivation of I_{CaT} increased maximum impedence amplitude. *C,* Increasing the inactivation time constant of I_{CaT} increased resonance strength. *D,* Increasing the inactivation time constant of I_{CaT} increased maximum impedence amplitude. All simulations were performed in the presence of a fixed magnitude of the *h* conductance.

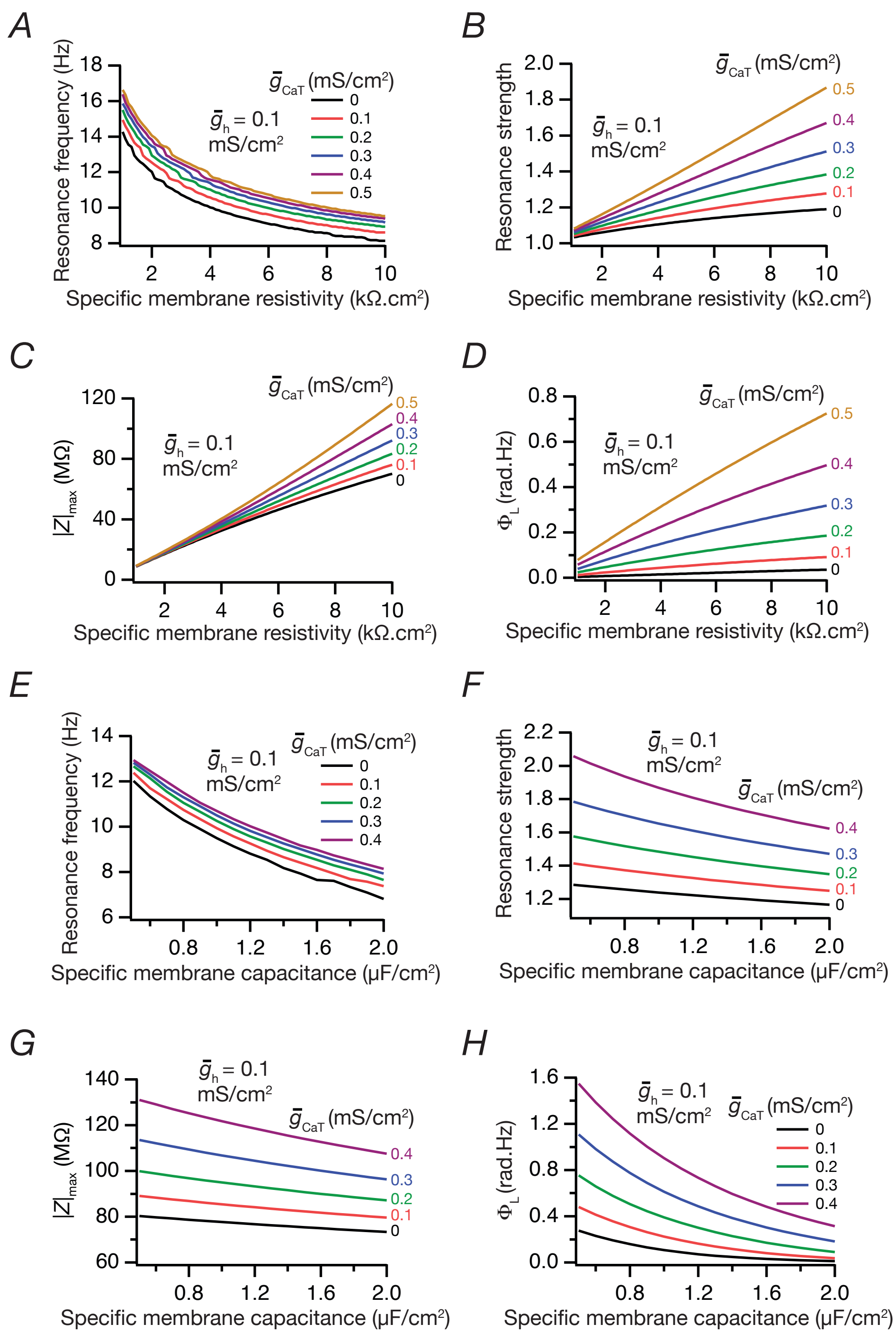

Supplementary Figure S13. Sensitivity analyses for passive parameters in determining intrinsic response dynamics in presence of *h* conductance and *T*-type Ca^{2+} conductance. *A,* An increase in membrane resistivity led to a reduction in resonance frequency, irrespective of presence of I_{CaT}. *B,* An increase in membrane resistivity led to an increase in resonance strength, irrespective of presence of I_{CaT}. *C,* An increase in membrane resistivity led to anincrease in maximum impedance amplitude, irrespective of presence of I_{CaT}. *D,* An increase in membrane resistivity led to an increase in total inductive phase, irrespective of presence of I_{CaT}. *E,* An increase in membrane capacitance led to a decrease in resonance frequency, irrespective of presence of I_{CaT}. *F,* An increase in membrane capacitance led to a decrease in resonance strength, irrespective of presence of I_{CaT}. *G,* An increase in membrane capacitance led to a decrease in maximum impedance amplitude, irrespective of presence of I_{CaT}. *H,* An increase in membrane capacitance led to a decrease in total inductive phase, irrespective of presence of I_{CaT}.

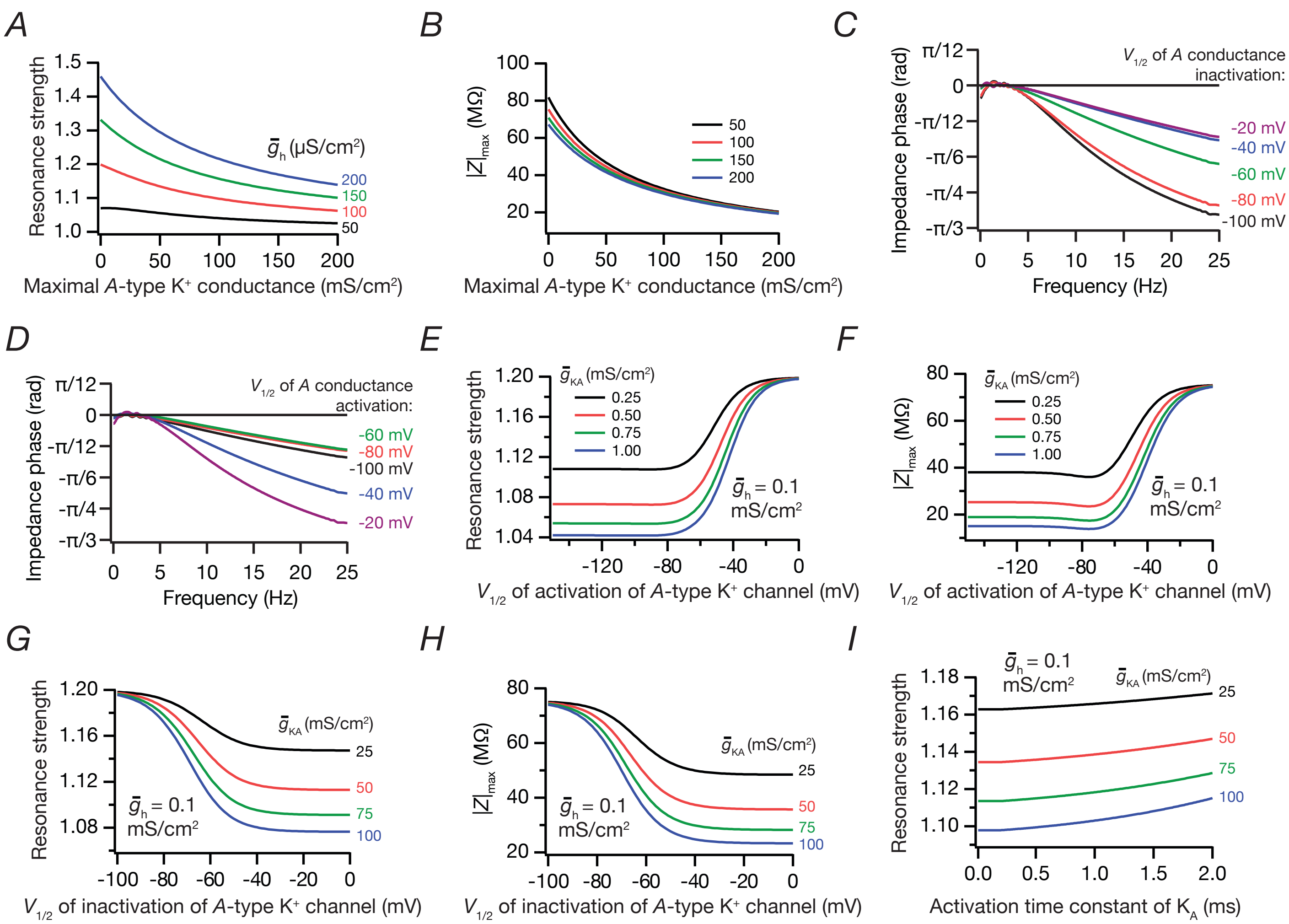

Supplementary Figure S14. Sensitivity analyses for the interactions between *h* conductance and active parameters of *A*-type K$^+$ conductance in determining resonance strength and maximum impedance amplitude. *A,* Increasing the magnitude of I_{KA} decreased resonance strength. *B,* Increasing the magnitude of I_{KA} decreased maximum impedance amplitude. *C–D,* Impedance amplitude plots for various half maximal inactivation (*C*) and activation (*D*) of I_{KA}. *E,* Depolarized shift in $V_{1/2}$ of activation of I_{KA} increased resonance strength. *F,* Depolarized shift in $V_{1/2}$ of activation of I_{KA} increased maximum impedance amplitude. *G,* Depolarized shift in $V_{1/2}$ of inactivation of I_{KA} decreased resonance strength. *H,* Depolarized shift in $V_{1/2}$ of inactivation of I_{KA} decreased maximum impedance amplitude. *I,* Increasing activation time constant of I_{KA} produced small increases in resonance strength. All simulations were performed in the presence of a fixed magnitude of the *h* conductance.

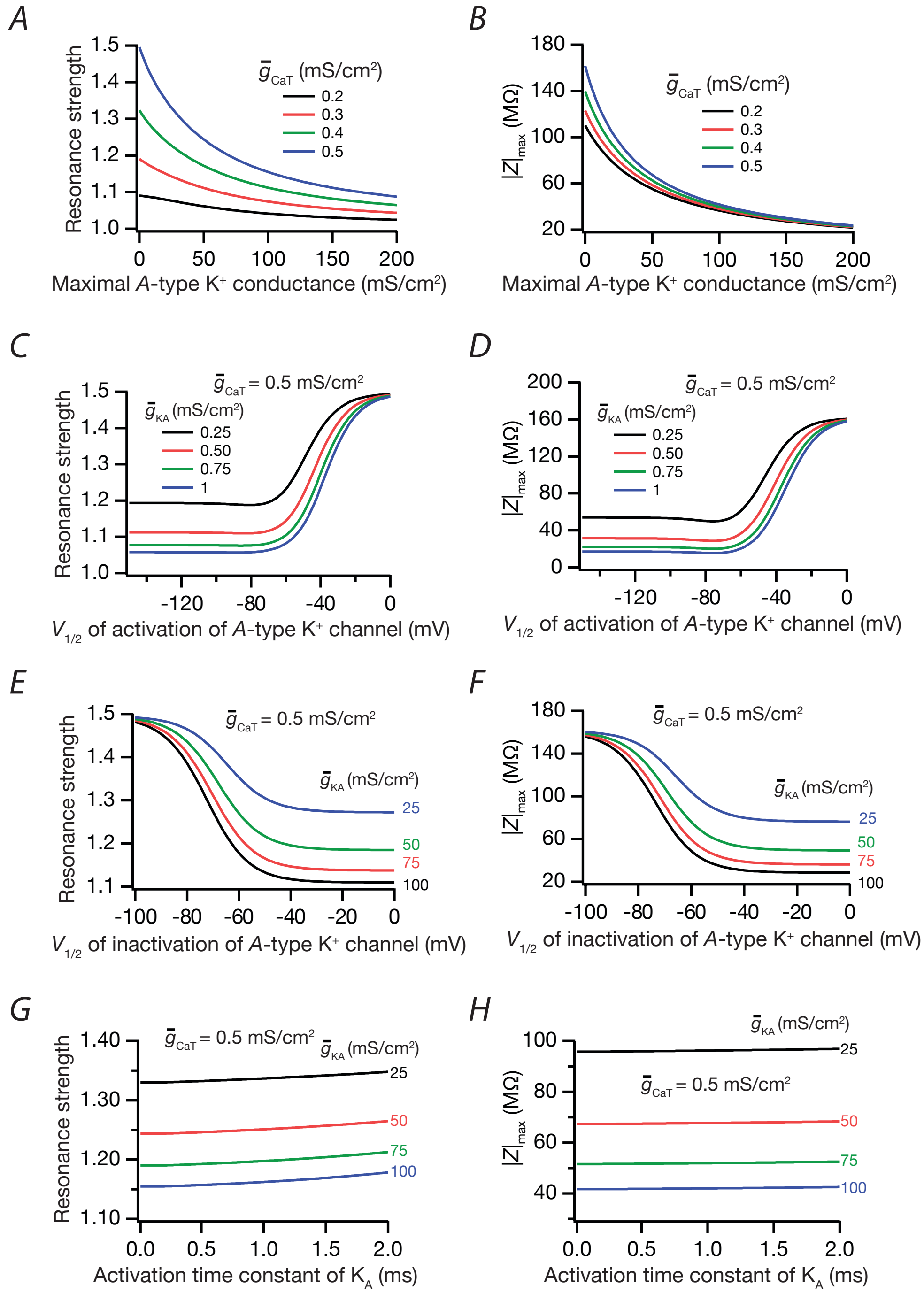

Supplementary Figure S15. Sensitivity analyses for the interactions between *T*-type Ca^{2+} conductance and active parameters of *A*-type K^+ conductance in determining resonance strength and maximum impedance amplitude. *A,* Increasing the magnitude of I_{KA} decreases resonance strength. *B,* Increasing the magnitude of I_{KA} decreased maximum impedance amplitude. *C,* Depolarized shift in $V_{1/2}$ of activation of I_{KA} increased resonance strength. *D,* Depolarized shift in $V_{1/2}$ of activation of I_{KA} increased maximum impedance amplitude. *E,* Depolarized shift in $V_{1/2}$ of inactivation of I_{KA} decreased resonance strength. *F,* Depolarized shift in $V_{1/2}$ of inactivation of I_{KA} decreased maximum impedance amplitude. *G,* Increasing activation time constant of I_{KA} produces small increased resonance strength. *H,* Increasing activation time constant of I_{KA} did not affect maximum impedance amplitude. All simulations were performed in the presence of a fixed magnitude of the *T* conductance.